

## ORIGINAL ARTICLE

**Characterization of hydroxyapatite containing a titania layer formed by anodization coupled with blasting**MIN-KYUNG KANG<sup>1</sup>, SEUNG-KYUN MOON<sup>1</sup>, JAE-SUNG KWON<sup>1,2</sup>,  
KWANG-MAHN KIM<sup>1,2</sup> & KYOUNG-NAM KIM<sup>1,2</sup><sup>1</sup>Research Center for Orofacial Hard Tissue Regeneration and Department and Research Institute of Dental Biomaterials and Bioengineering, and <sup>2</sup>Brain Korea 21 PLUS Project, Yonsei University College of Dentistry, Seoul, Republic of Korea**Abstract**

**Objectives.** The modification of dental implant surface by increasing the surface roughness or/and altering chemical composition have been attempted. Among them, hydroxyapatite (HA) coatings are typically bioactive. On the other hand, titania coatings have good corrosion resistance and biocompatibility. Therefore, the objective of this study was to fabricate HA containing a titania layer using an HA blasting and anodization method to benefit from the advantages of both, followed by surface characterization and biocompatibility. **Materials and methods.** HA blasting was performed followed by microarc oxidation (MAO) using various applied voltages (100, 150, 200, 250 V). For surface characterization, the microstructure of the surface, surface phase and surface roughness were observed. Bonding strength was measured using a universal testing machine and potentiodynamic corrosion testing was performed. Biocompatibility was evaluated based on bioactivity and cell proliferation test. **Results.** The porous titanium oxide-containing HA was formed at 150 and 200 V. These surfaces were a lower corrosion current compared to the titanium treated only with HA blasting. In addition, composite treated titanium showed a rougher surface and tighter bonding strength compared to the titanium treated only with MAO. Biocompatibility demonstrated that HA/Titania composite layer on titanium showed a rapid HA precipitation and also enhanced cell proliferation. **Conclusions.** These results suggested that HA containing titania layer on titanium had not only excellent physicochemical, mechanical and electrochemical properties, but also improved bioactivity and biological properties that could be applied as material for a dental implant system.

**Key Words:** *anodization, blasting, dental implant, hydroxyapatite, titania***Introduction**

The clinical success of oral implants is dependent on the duration of the treatment periods which is improved by the rapid osseointegration [1]. The rate and quality of osseointegration in titanium implants are related to their surface properties. Therefore, many studies have targeted improving the bone–implant interface, with the aim of accelerating bone healing and improving bone anchorage to the implant, typically following two approaches [2,3]. In the first approach, the surface is modified physically by way of the architecture of the surface topography. Surface topography depends on surface orientation and roughness [4]. To obtain a rough surface, grit blasting, acid-etching and anodization have been

introduced [3,5]. The anodization method yields a good implant corrosion resistance and biocompatibility. In addition, a specific anodization method, such as novel silicone-based electrochemical treatment on titanium, has shown to even improve bioactivity [6]. In the second approach, the surface is improved chemically by incorporation of osteoconductive calcium phosphate such as using for plasma spraying, sol-gel coating, electrophoretic deposition and biomimetic precipitation which has been shown to be effective [7–10]. Following implantation, the release of calcium phosphate into the peri-implant region increases the saturation of body fluid and precipitates a biological apatite onto the surface of the implant [11]. The biological fixation of a titanium implant to bone tissue is shown to be faster with a calcium

---

Correspondence: Kyoung-Nam Kim, Research Center for Orofacial Hard Tissue Regeneration and Department and Research Institute of Dental Biomaterials and Bioengineering, Yonsei University College of Dentistry, 50-1 Yonsei-ro, Seodaemun-gu, Seoul 120-752, Republic of Korea. Tel: +82 2 2228 3081. Fax: +82 2 364 9961. E-mail: kimkn@yuhs.ac

(Received 11 February 2014; accepted 28 May 2014)

ISSN 0001-6357 print/ISSN 1502-3850 online © 2014 Informa Healthcare  
DOI: 10.3109/00016357.2014.933484

phosphate coating than without [12,13]. These methods typically yield bioactive implants, but adhesion strength to the substrate is poor. Recently, many researchers have tried to combine the physical and chemical modification of the surface using materials such as HA containing a titania composite coating to benefit from the advantages of both approaches [6,14].

So, the aim of this study was to form HA containing a titania layer resulting from HA blasting and anodization, processed under different voltage conditions. Further, the HA containing a titania layer on titanium was evaluated for surface characteristics and biocompatibility.

## Materials and methods

### Preparation of specimens

Commercially pure titanium (cp-Ti, grade III, ASTM F67) was used for the specimens ( $10 \times 10 \times 0.5 \text{ mm}^3$ ). Fabrication of the HA/titania composite layer involved a three-step process. First, the titanium surface was mechanically polished using an ECO-MET polisher (Buehler, Lake Bluff, IL) with SiC paper with grits of 100, 600 and 1200. Second, titanium was grit blasted using a grit blasting machine (DUST INN 2000, Deldent, Windsor, CT) at a pressure of 4 bars. The voltage of the power supply was 12 V DC, while the distance between specimen and blaster tip was set to 10 mm. The hydroxyapatite powder with the size between 45 and 180  $\mu\text{m}$  (MCD Powder, Himed, New York, NY) was used to grit blast. The titanium was then cleaned ultrasonically in distilled water for 5 min. Finally, titanium was anodized at four different voltages from 100–250 V for 3 min with a DC power supply (Genesys 600-2.6, Densi-Lambda, Tokyo, Japan). A mixed solution of 0.4 M calcium acetate n-hydrate ( $\text{C}_2\text{H}_3\text{O}_2\text{Ca}\cdot n\text{H}_2\text{O}$ , Junsei, Tokyo, Japan) and 0.04 M beta-glycerol phosphate disodium salt n-hydrate ( $\text{C}_3\text{H}_7\text{Na}_2\text{O}_6\text{P}\cdot n\text{H}_2\text{O}$ , Fluka, Buch, Switzerland) was used as an electrolyte [15]. The experimental groups were sorted according to the surface treatment and are listed in Table I.

### Analysis of surface characteristics

The surface morphology was observed using field-emission scanning electron microscopy (FE-SEM; JSM-6700F, JEOL, Tokyo, Japan). For the crystalline phase analysis, the surface layer was analyzed by high-resolution X-ray diffraction (XRD; Bruker D8 DISCOVER, Bruker, Germany) using the  $\text{K}\alpha$  radiation of the Cu target in the scan range of  $10\text{--}80^\circ$  at a scan rate of  $2^\circ/\text{min}$ . Surface roughness of coating layer was measured with surface profiler (Microfilm Reader, Kosaka Laboratory Ltd, Tokyo, Japan). Three measurements were performed on each specimen to

Table I. Experimental groups according to surface treatment.

Group	Method
SM	Polishing
HA	Polishing + HA blasting
MAO	Polishing + Anodization 250 V
HA + MAO 100	Polishing + HA blasting + Anodization 100 V
HA + MAO 150	Polishing + HA blasting + Anodization 150 V
HA + MAO 200	Polishing + HA blasting + Anodization 200 V
HA + MAO 250	Polishing + HA blasting + Anodization 250 V

SM, simple machine; HA, hydroxyapatite; MAO, macroarc oxidation.

evaluate the average of surface roughness (Ra) values where the drive speed was set to 0.1 mm/s. The bonding strength between the coated layer and substrate was measured using a universal testing machine (3366, Instron, Norwood, MA) by attaching one side of the specimen to a cylindrical stainless steel rod (10 mm diameter, 30 mm height) using an adhesive glue (Loctite E-214HP Hysol, A.T. Chemical, Seoul, Korea) and measuring the tensile bonding strength. The cross-head speed of the universal testing machine was set to 1 mm/min ( $n = 15$ ) and the fractured surfaces of the specimens were observed by both FE-SEM and energy-dispersive X-ray spectroscopy (EDS; Inca program, Oxford, UK) after the bonding test. To evaluate the corrosion resistance, potentiodynamic testing was performed in artificial saliva at  $37^\circ\text{C}$ , while the composition of the artificial saliva is listed in Table II [16]. In the case of the corrosion cell (K0047 Princeton Applied Research, Oak Ridge, TN, USA), a platinum electrode was used as an auxiliary electrode and a saturated calomel electrode (SCE) was used as the reference electrode. The area exposed to the saliva was  $1.0 \text{ cm}^2$  by installing the specimen to a flat specimen holder kit (K0105 Princeton Applied Research, Oak Ridge, TN, USA) which allowed only one surface of  $1 \text{ cm} \times 1 \text{ cm}$  which was exposed to artificial saliva. The potential scanning rate was 1 mV/s, and the scanning range was  $-1000$  to  $2000 \text{ mV}$  (SCE) ( $n = 5$ ).

Table II. Constituents of artificial saliva [16].

Constituent	Concentration
NaCl, g/l	0.40
KCl, g/l	0.40
$\text{CaCl}_2\cdot 2\text{H}_2\text{O}$ , g/l	0.795
$\text{NaH}_2\text{PO}_4\cdot 2\text{H}_2\text{O}$ , g/l	0.78
$\text{Na}_2\text{S}\cdot 9\text{H}_2\text{O}$ , g/l	0.005
$\text{CO}(\text{NH}_2)_2$ (Urea), g/l	1.0
Distilled water, ml	1000

Table III. Ion concentrations of simulated fluid and human plasma [17].

Ion	Ion concentrations (mM)	
	Blood plasma	SBF
Na <sup>+</sup>	142.0	142.0
K <sup>+</sup>	5.0	5.0
Mg <sup>2+</sup>	1.5	1.5
Ca <sup>+</sup>	2.5	2.5
Cl <sup>-</sup>	103.0	147.8
HCO <sub>3</sub> <sup>-</sup>	27.0	4.2
HPO <sub>4</sub>	1.0	1.0
SO <sub>4</sub> <sup>2-</sup>	0.5	0.5
pH	7.2–7.4	7.40

### Biocompatibility

The bioactivity test was performed by immersion of specimen in simulated body fluid (SBF) that was prepared by dissolving reagent chemicals of NaCl,

NaHCO<sub>3</sub>, KCl, K<sub>2</sub>HPO<sub>4</sub>·3H<sub>2</sub>O, MgCl<sub>2</sub>·6H<sub>2</sub>O, CaCl<sub>2</sub> and Na<sub>2</sub>SO<sub>4</sub> into deionized water. Ionic concentration of SBF was approximately the same as that of human blood plasma, as reported in Table III [17]. Each specimen was immersed in SBF solution at 100 rpm in a shaking incubator at 37°C for 7 and 14 days. After the immersion, the specimen was rinsed in the distilled water and dried, while the morphology of the precipitates on the specimens was observed by FE-SEM.

For evaluation of cell compatibility, MC3T3-E1 cells (mouse osteoblastic cells, ATCC, Manassas, VA, USA) with passages between 5–15, were used. Cells were grown in  $\alpha$ -MEM medium ( $\alpha$ -MEM, Gibco, Carlsbad, CA, USA) containing 10% fetal bovine serum (Gibco) and penicillin/streptomycin. Cultures were incubated in a humidified atmosphere of 5% CO<sub>2</sub> at 37°C. The cells were seeded onto the specimens at a density of  $5 \times 10^4$  cells/mL in the medium. Seeded specimens were incubated in a CO<sub>2</sub> incubator (5% CO<sub>2</sub>, 37°C). After 4, 24 and 72 h, cell proliferation was determined using the methylthiazol tetrazolium (MTT) assay.

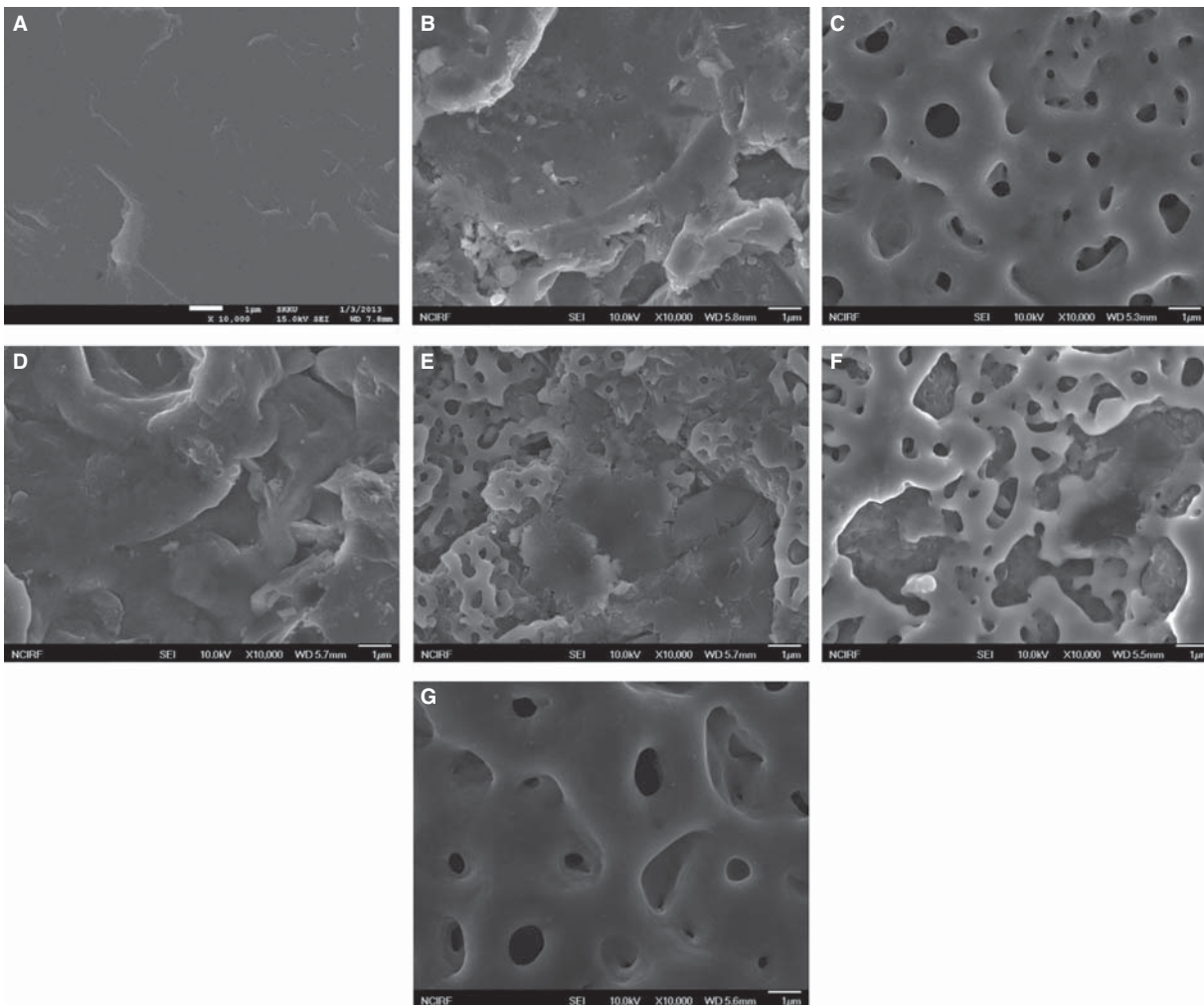


Figure 1. FE-SEM image of a modified surface formed on the cp-Ti ( $\times 10\,000$ ). (A) SM, (B) HA, (C) MAO, (D) HA + MAO 100, (E) HA + MAO 150, (F) HA + MAO 200 and (G) HA + MAO 250.

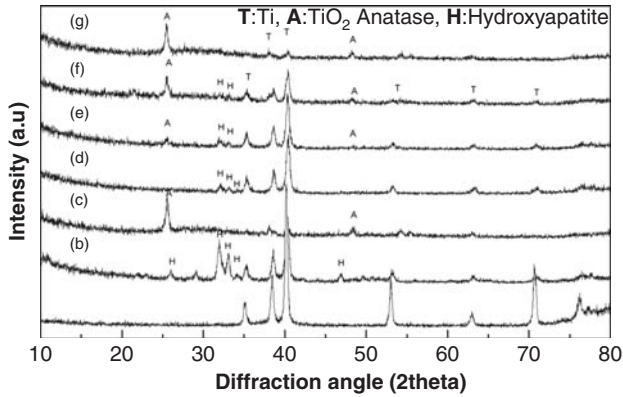


Figure 2. XRD pattern of the modified surface formed on the cp-Ti. (A) SM, (B) HA, (C) MAO, (D) HA + MAO 100, (E) HA + MAO 150, (F) HA + MAO 200 and (G) HA + MAO 250.

### Statistical analysis

Differences in the results of surface roughness, bonding strength and cell proliferation were analyzed using one-way ANOVA, with Tukey's test for the post-hoc analysis. The significance level was set at 95%.

## Results

### Surface characterization

Figure 1 shows the morphology of the specimens. The HA and titania composite layer was formed at HA + MAO 150 and HA + MAO 200, while the porous oxide layer and HA structure were formed concurrently (Figures 1E and F). From the results of phase identification (Figure 2), anatase and HA peaks could be observed on HA + MAO 150 and HA + MAO 200 (Figures 2E and F).

The results of surface roughness measurement are presented in Table IV. The average surface roughness value (Ra) decreased in the following order: HA + MAO 100 (1.03  $\mu\text{m}$ ) > HA (1.01  $\mu\text{m}$ ) > HA + MAO 150 (0.99  $\mu\text{m}$ ) > HA + MAO 200 (0.95  $\mu\text{m}$ ) > HA + MAO 250 (0.80  $\mu\text{m}$ ) > MAO (0.37  $\mu\text{m}$ ) > SM (0.18  $\mu\text{m}$ ).

Table IV. Average surface roughness value of the modified surface formed on the cp-Ti.

Group	Mean ( $\mu\text{m}$ ) ( $\pm\text{SD}$ )
SM	0.18 <sup>a</sup> ( $\pm 0.01$ )
HA	1.01 <sup>b</sup> ( $\pm 0.05$ )
MAO	0.37 <sup>a</sup> ( $\pm 0.11$ )
HA + MAO 100	1.03 <sup>b</sup> ( $\pm 0.16$ )
HA + MAO 150	0.99 <sup>b</sup> ( $\pm 0.14$ )
HA + MAO 200	0.95 <sup>b</sup> ( $\pm 0.12$ )
HA + MAO 250	0.80 <sup>c</sup> ( $\pm 0.02$ )

a, b, c values with the same letters showed no significant differences ( $p > 0.05$ ).

In the bonding test (Figure 3), HA showed the highest bonding strength, but there were no significant differences among the HA + MAO 100, HA + MAO 150 and HA + MAO 200 ( $p > 0.05$ ). In addition, Figure 4 shows all specimens after the bonding test. The HA, HA + MAO 100, HA + MAO 150 and HA + MAO 200 showed a very low contents of Ti, O, Ca, P and C of glue component that indicate that bonding failure was in a form of cohesive failure (Figures 4A–C, G–I, J–L and M–O). However, MAO and HA + MAO 250 showed a pattern of adhesive failure as the only Ti substrate components were observed on the surface following the bonding test (Figures 4D–F and P–R).

According to the values of  $I_{\text{cor}}$  (Figure 5), the corrosion resistance of the specimens was ranked as follows: MAO > HA + MAO 250 > HA + MAO 200 > HA + MAO 150 > HA + MAO 100 > SM > HA. Thus, the HA/titania composite layered titanium showed better corrosion resistance in artificial saliva than SM and HA.

### Biocompatibility

Figure 6 shows the surface morphologies after immersion in SBF for 7 days. After 7 days, apatite of the needle structure showed on the HA, HA + MAO 100, HA + MAO 150 and HA + MAO 200 (Figures 6C, D and G–L). However, area of the apatite on the HA + MAO 200 (Figures 6K and L) appeared to be smaller than the surface of HA, HA + MAO 100 and HA + MAO 150. The surface on SM, MAO and HA + MAO 250 could not observed apatite structure (Figures 6A, B, E, F, M and N). Figure 7 shows the surface morphologies after immersion in SBF for 14 days. After immersion in SBF for 14 days, SEM image showed apatite like structures covering the whole surface of titanium treated with HA, HA + MAO 100, HA + MAO 150 and HA + MAO 200 (Figures 7C, D and G–L). In contrast, only part of the surface was covered with apatite on SM, MAO and HA + MAO 250 (Figures 7A, B, E, F, M and N).

Figure 8 shows the cellular proliferation of MC3T3-E1 cells at 4, 24 and 72 h after cell seeding. At 4 h, the highest cell proliferation was identified on HA; however, there were no significant differences among MAO, HA + MAO 100, HA + MAO 150, and HA + MAO 200 ( $p > 0.05$ ). At 24 and 72 h, there was significantly increased cellular proliferation on HA + MAO 150, HA + MAO 200 and HA + MAO 250 ( $p < 0.05$ ).

## Discussion

### Surface characterization

Figure 1 shows the morphologies of the specimens. As the SEM images indicate, the applied voltage

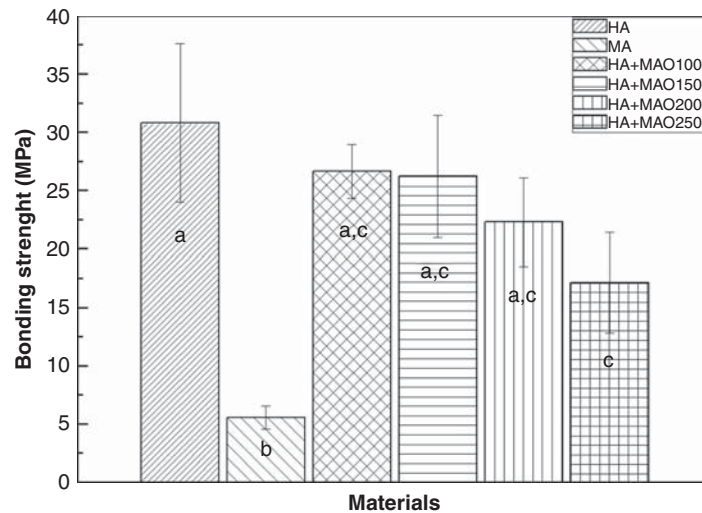


Figure 3. Bonding strength between the coated layer and Ti substrate. (A) HA, (B) MAO, (C) HA + MAO 100, (D) HA + MAO 150, (E) HA + MAO 200 and (F) HA + MAO 250. (A–C: bars with the same letters showed no significant differences ( $p > 0.05$ )).

decreased as more HA particle structures were exposed on the surface. HA + MAO 100 was similar to HA, which was fully covered HA. HA + MAO 250 was similar to the morphology of MAO. HA + MAO 150 and HA + MAO 200 exhibited an HA structure and a porous oxide layer together. The oxide thickness and formation were related to the applied voltage and the oxide thickness was less than 1  $\mu\text{m}$  at 100–200 V. When applied voltages were above 250 V, the oxide thickness was 2–3  $\mu\text{m}$  [18,19]. Thus, the HA particle could partially be exposed on the HA + 150 and HA + 200 surfaces, but HA particles were covered with a thick oxide layer on the HA + MAO 250.

These HA and titania components of the surface were confirmed by XRD results. As Figure 2 shows, the HA/titania composite layer on titanium exhibited anatase and HA peaks together. Based on results for the HA layer, there were no compositional or crystallographic changes resulting from anodization after blasting treatment. The HA blasting method thus has significant advantages over plasma spray, which often result in compositional change as well as the crystallinity due to the extremely high temperature during the process. Also, it is worth noting that the character of HA in the coating from plasma spray differs from HA found in the bone; the crystallinity of HA in the coating is extremely high, while that of HA from bone is low [11,20]. The titania has three stable forms: rutile, anatase and brookite. Increasing the thickness usually increases crystallinity [21]. Compared to rutile titania, anatase titania has unique properties and advantages for medical application, such as exhibiting stronger interactions between the metal and support compared to rutile [22–25]. In the present study, the intensity of the anatase peak increased with the applied voltage.

Measurement of the roughness parameter of the dental implant surface morphology is important

because its value influences the adhesion, adsorption and differentiation of the cell. The high roughness of the implant surface results in mechanical interlocking between the implant surface and bone. The most commonly used dental implant roughness parameter is  $R_a$ , the arithmetic medium value of the deviations of the roughness profile in relation to a medium line [26]. In this study, the highest  $R_a$  value was identified in HA + MAO 100. However, there were no significant differences in  $R_a$  values among HA, HA + MAO 150 and HA + MAO 200 ( $p > 0.05$ ). Also the lowest  $R_a$  value was found in SM ( $p < 0.05$ ). These results indicated that blasting methods increase the surface roughness due to a subtractive process, such as the etching process.

The delamination of the implant coating layer is a serious biocompatibility concern because it causes release of undesirable debris into the biological environment, resulting in implant failure. Therefore, the stability of the coating layer is an important parameter for implant success. In this study, the bonding strength was carried out, which showed that the value can be increased with HA blasting treatment. Ishikawa and Ogino [25] speculated two types of mechanism of blast coating on the titanium surface, one of which was mechanical interlocking [25]. In this way, HA powder could become embedded in the titanium. The second type of bonding was between the HA particles themselves. The blasting method results in intense collisions not only between HA particles and titanium, but also between HA particles themselves. These mechanisms also were demonstrated by the results of surface roughness. As mentioned earlier, the blasting process was shown to increase the surface roughness through  $R_a$  value and such results are expected to have influenced the bonding strength results. Furthermore, poor adhesion of MAO 250 may also be related to the thicker oxide layer obtained

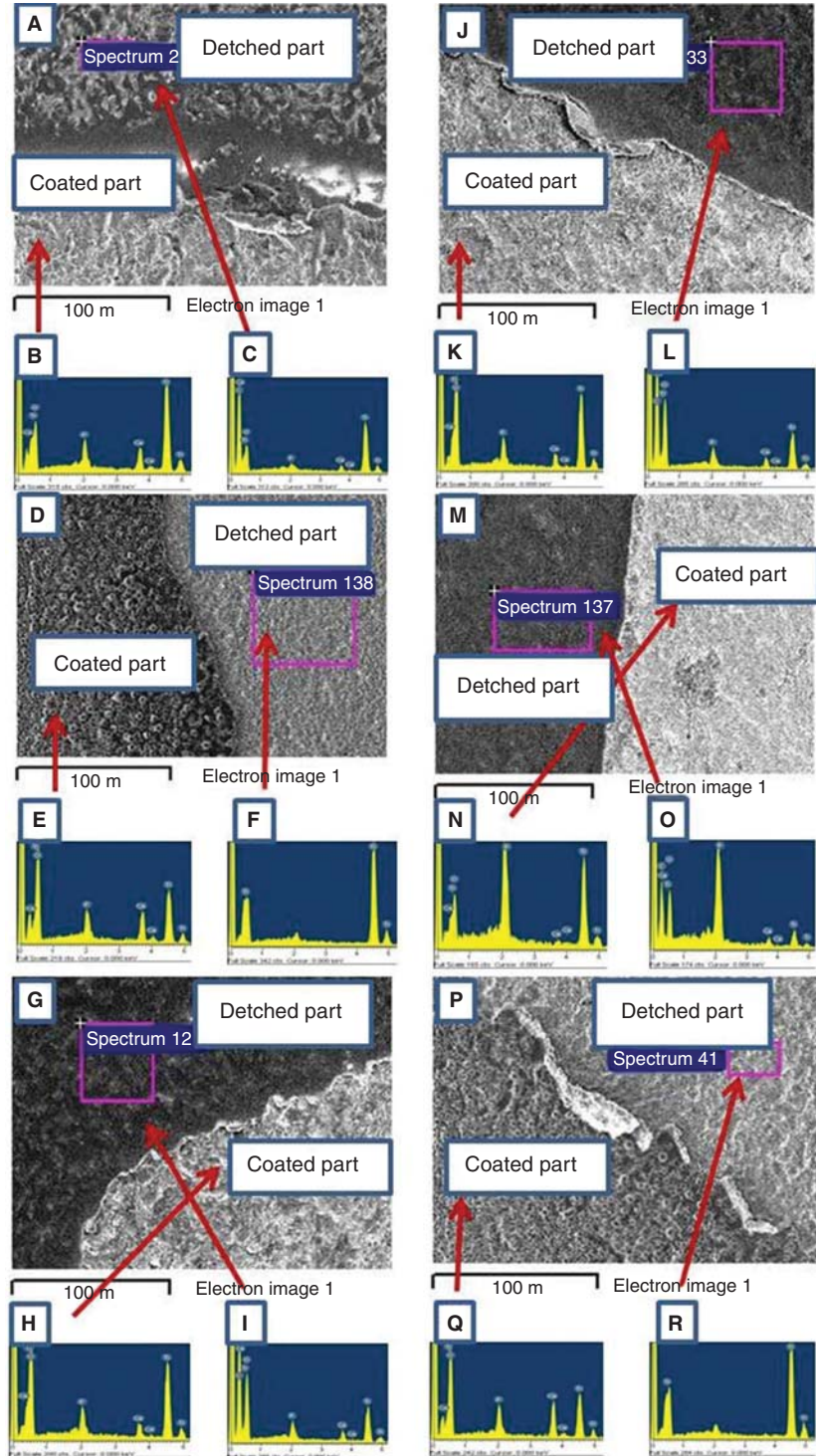


Figure 4. SEM and EDS of the fractured surfaces of (A–C) HA, (D–F) MAO, (G–I) HA + MAO 100, (J–L) HA + MAO 150, (M–O) HA + MAO 200 and (P–R) HA + MAO 250.

due to higher processing voltage. Therefore, results for cohesive fractured HA, HA + MAO 100, HA + MAO 150 and HA + MAO 200 indicated that blasting treatment could improve bonding strength because of mechanical interlocking and mechanochemical bonding. In contrast, MAO and HA + MAO 250 showed adhesive failure, suggesting weak bonding strength and fracture between the coated layer and substrate.

Corrosion behavior is important because poor biocompatibility and toxicity of material may be adverse for implantation purposes. Therefore, many studies have examined various surface treatments for forming a more homogeneous and dense oxide layer [27]. Cigada et al. [28] investigated the oxide films formed by anodization with different thicknesses on titanium and titanium alloy. Their studies indicated that higher oxide thickness on titanium or titanium

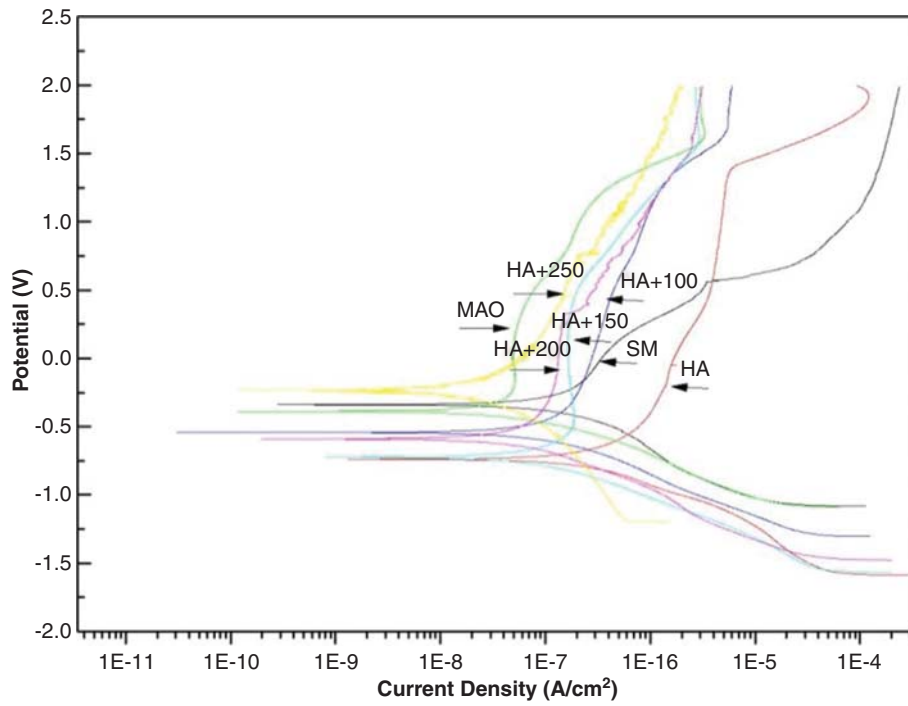


Figure 5. Anodic polarization curves of the modified titanium.

alloy could significantly reduce the passivity current in a physiological solution of titanium. In the present study, MAO showed the lowest current density and,

thus, had the best corrosion resistance, possibly due to the increased oxide thickness. Also, HA containing anodized titania-layered titanium (HA + MAO 100,

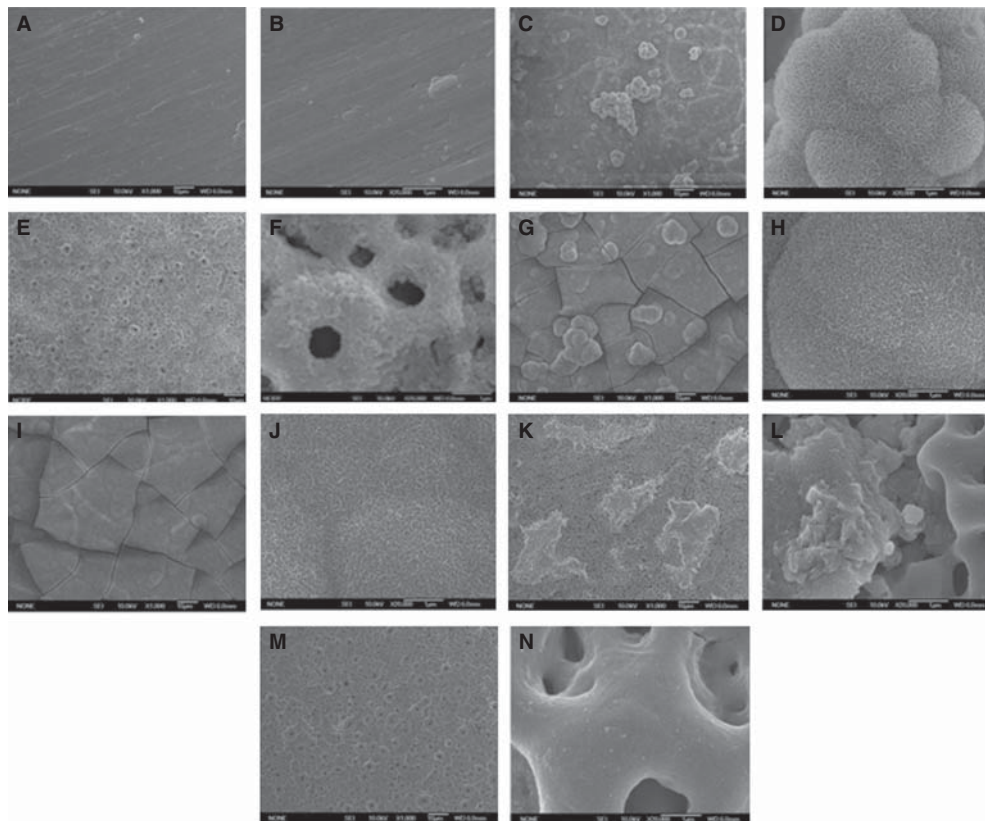


Figure 6. Surface morphologies of the specimen soaked in SBF for 7 days ( $\times 1000$ ,  $20\,000$ ). (A, B) SM, (C, D) HA, (E, F) MAO, (G, H) HA + MAO 100, (I, J) HA + MAO 150, (K, L) HA + MAO 200 and (M, N) HA + MAO 250.

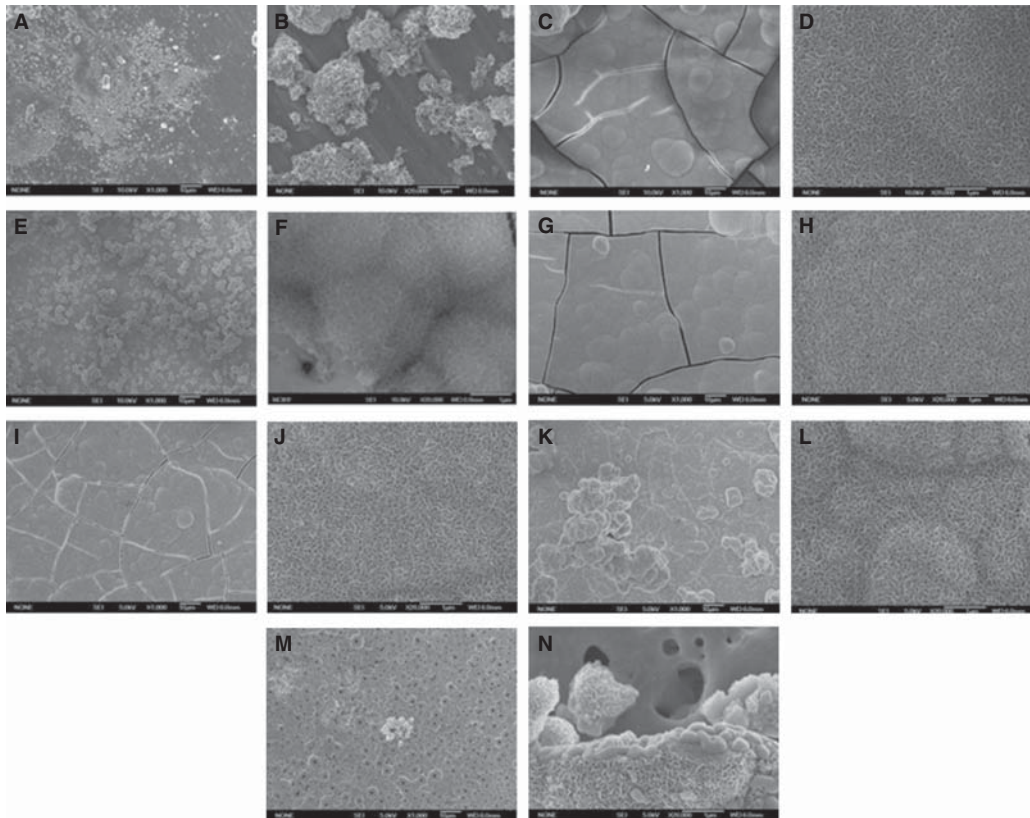


Figure 7. Surface morphologies of the specimen soaked in SBF for 14 days ( $\times 1000$ , 20 000). (A, B) SM, (C, D) HA, (E, F) MAO, (G, H) HA + MAO 100, (I, J) HA + MAO 150, (K, L) HA + MAO 200 and (M, N) HA + MAO 250.

HA + MAO 150 and HA + MAO 200) showed better corrosion resistance than SM and HA due to the thicker oxide layer, while the blasted titanium had the highest current density, resulting in the worst corrosion resistance.

*Biocompatibility*

The apatite forming ability of implants appears to be correlated with their biocompatibility *in vivo* [29,30]. After the bioactivity test, the result indicated that HA

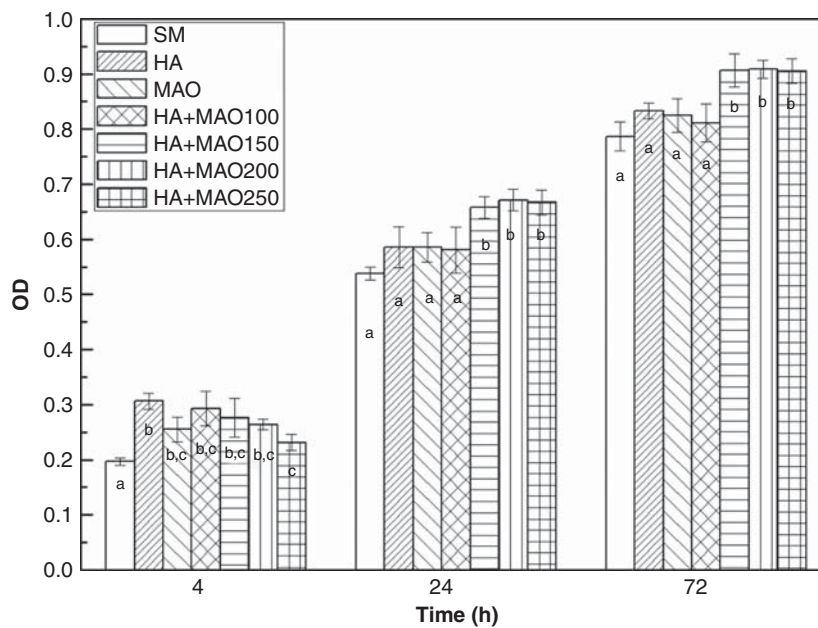


Figure 8. Proliferation of MC3T3-E1 cells on the modified titanium. (A–C: bars with the same letters showed no significant differences ( $p > 0.05$ )).

containing titania layered titanium (HA + MAO 100, HA + MAO 150, HA + MAO 200) showed more rapid and better bioactivity as showing early precipitation of apatite compared to only the polished (SM) and anodized surface (MAO). In another study, apatite was not formed on anodized titanium, even though anatase was also present on the surface. This study suggested that apatite formation on titanium can be attained by anodic oxidation in conjunction with heat treatment or hydrothermal treatment [31,32]. Also, similar to the effects seen by the anodization process such as novel silicone-based electrochemical treatment [6], this study showed that HA blasted titanium and HA containing titania layered titanium improved bioactivity of the material. HA is well known for a good bioactivity material. The chemical composition of HA such as Ca, P is similar with bone tissue. Therefore, HA blasted surface could induce the osteoinduction [33]. Additionally, the chemical factor of the surface and surface morphology may have effects on the bioactivity. The rough surface could provide more spaces for seeding on the metal surface with calcium phosphate nuclei [34,35]. So, the growth rate of apatite could be accelerated by HA blasting treatment.

The efficiency of cell proliferation was determined using the MTT assay. Figure 8 shows the cellular proliferation of MC3T3-E1 cells at 4, 24 and 72 h after cell seeding. For all incubation times, SM showed the lowest cell proliferation, while HA + MAO 150 and HA + MAO 200 were associated with excellent proliferation. Surface topography and roughness are known to affect cell proliferation [36]. However, surface free energy such as wettability is more important than surface roughness for cellular adhesion and proliferation [37]. An anodized surface is known to be hydrophilic [36], while the HA + MAO250 is both hydrophilic as well as somewhat rough on the surface. Thus, HA + MAO250 showed higher cell proliferation than HA after 24 and 72 h. In addition, surface composition should also be considered a factor in cell proliferation. The surface-incorporated Ca and P ions were also associated with enhanced cell proliferation. The observed positive effect may be the result of release of Ca and/or P ions or molecules that can penetrate the cell membrane or activate membrane-bound receptors [38]. In this study, HA containing titania layered titanium had more Ca and P compared with SM and MAO.

## Conclusion

From the above results, the HA containing a titania composite layer on titanium, especially HA + MAO 150 and HA + MAO 200, demonstrated improved bonding strength and bioactivity, achieved using the HA blasting method of surface treatment, whereas corrosion resistance was improved by anodization. Cell compatibility was also improved by HA blasting

coupled with anodization. Therefore, these results indicate that HA containing a titania composite layer on titanium not only has excellent physical, mechanical and electrochemical properties, but also exhibits improved biocompatibility and, thus, could be useful as material for dental implant systems.

## Acknowledgments

This work was supported by a grant from the National Research Foundation of Korea (NRF), which was funded by the Korean Government (MSIP) (NRF-2010-0027963).

**Declaration of interest:** The authors report no conflicts of interest. The authors alone are responsible for the content and writing of the paper.

## References

- [1] Albrektsson J. Osteoinduction, osteoconduction and osseointegration. *Eur Spine J* 2001;10:S96–S101.
- [2] Dohan Ehrenfest DM, Coelho PG, Kang BS, Sul YT, Albrektsson T. Classification of osseointegrated implant surfaces: materials, chemistry and topography. *Trends Biotechnol* 2010;28:198–206.
- [3] Le Guéhennec L, Soueidan A, Layrolle P, Amouriq Y. Surface treatments of titanium dental implants for rapid osseointegration. *Dent Mater* 2007;23:844–54.
- [4] Wennerberg A, Albrektsson T. Effects of titanium surface topography on bone integration: a systematic review. *Clin Oral Implants Res* 2009;20:172–84.
- [5] Coelho PG, Granjeiro JM, Romanos GE, Suzuki M, Silva NRF, Cardaropoli G, et al. Basic research methods and current trends of dental implant surfaces. *J Biomed Mater Res B* 2009;88B:579–96.
- [6] Della Valle C, Rondelli G, Cigada A, Edoardo Bianchi A, Chiesa R. A novel silicon-based electrochemical treatment to improve osteointegration of titanium implants. *J Appl Biomater Funct Mater* 2013;11:106–16.
- [7] Ban S, Maruno S. Effect of temperature on electrochemical deposition of calcium phosphate coatings in a simulated body fluid. *Biomaterials* 1995;16:977–81.
- [8] Lee J, Aoki H. Hydroxyapatite coating on Ti plate by a dipping method. *Biomed Mater Eng* 1995;5:49–58.
- [9] Ishikawa K, Miyamoto Y, Nagayama M, Asaoka K. Blast coating method: new method of coating titanium surface with hydroxyapatite at room temperature. *J Biomed Mater Res* 1997;38:129–34.
- [10] Ban S, Maruno S, Arimoto N, Harada A, Hasegawa J. Effect of electrochemically deposited apatite coating on bonding of bone to the HA-G-Ti composite and titanium. *J Biomed Mater Res* 1997;36:9–15.
- [11] Daculsi G, Laboux O, Malard O, Weiss P. Current state of the art of biphasic calcium phosphate bioceramics. *J Mater Sci Mater Med* 2003;14:195–200.
- [12] Morris HF, Ochi S, Spray JR, Olson JW. Periodontal-type measurements associated with hydroxyapatite-coated and non-HA-coated implants: uncovering to 36 months. *Ann periodontol* 2000;5:56–67.
- [13] Barrère F, Van Der Valk CM, Meijer G, Dalmeijer RAJ, De Groot K, Layrolle P. Osteointegration of biomimetic apatite coating applied onto dense and porous metal implants in femurs of goats. *J Biomed Mater Res B Appl Biomater* 2003;67:655–65.

- [14] Chiesa R, Giavaresi G, Fini M, Sandrini E, Giordano C, Bianchi A, et al. In vitro and in vivo performance of novel surface treatment to enhance osseointegration of endosseous implants. *Oral Surg Oral Med Oral Pathol Oral Radiol Endod* 2007;103:745–56.
- [15] Zhu X, Kim KH, Jeong Y. Anodic oxide films containing Ca and P of titanium biomaterial. *Biomaterials* 2001;22:2199–206.
- [16] Shim HM, Oh KT, Woo JY, Hwang CJ, Kim KN. Corrosion resistance of titanium-silver alloys in an artificial saliva containing fluoride ions. *J Biomed Mater Res Part B Appl Biomater* 2005;73B:252–9.
- [17] Kunze J, Müller L, Macak JM, Greil P, Schmuki P, Müller FA. Time-dependent growth of biomimetic apatite on anodic TiO<sub>2</sub> nanotubes. *Electrochim Acta* 2008;53:6995–7003.
- [18] Velten D, Biehl V, Aubertin F, Valeske B, Possart W, Breme J. Preparation of TiO<sub>2</sub> layers on cp-Ti and Ti6Al4V by thermal and anodic oxidation and by sol-gel coating techniques and their characterization. *J Biomed Mater Res* 2002;59:18–28.
- [19] Li LH, Kong YM, Kim HW, Kim YW, Kim HE, Heo SJ, et al. Improved biological performance of Ti implants due to surface modification by micro-arc oxidation. *Biomaterials* 2004;25:2867–75.
- [20] Cheang P, Khor KA. Addressing processing problems associated with plasma spraying of hydroxyapatite coatings. *Biomaterials* 1996;17:537–44.
- [21] Diebold U. The surface science of titanium dioxide. *Surf Sci Rep* 2003;48:53–229.
- [22] Akin FA, Zreiqat H, Jordan S, Wijesundara MJB, Hanley L. Preparation and analysis of macroporous TiO<sub>2</sub> films on Ti surfaces for bone-tissue implants. *J Biomed Mater Res* 2001;57:588–96.
- [23] Yerokhin AL, Nie X, Leyland A, Matthews A. Characterisation of oxide films produced by plasma electrolytic oxidation of a Ti-6Al-4V alloy. *Surf Coat Tech* 2000;130:195–206.
- [24] Nie X, Leyland A, Matthews A, Jiang JC, Meletis EI. Effects of solution pH and electrical parameters on hydroxyapatite coatings deposited by a plasma-assisted electrophoresis technique. *J Biomed Mater Res* 2001;57:612–18.
- [25] Ishizawa H, Ogino M. Formation and characterization of anodic titanium oxide films containing Ca and P. *J Biomed Mater Res* 1995;29:65–72.
- [26] Elias CN, Oshida Y, Lima JHC, Muller CA. Relationship between surface properties (roughness, wettability and morphology) of titanium and dental implant removal torque. *J Mech Behav Biomed Mater* 2008;1:234–42.
- [27] Park IS, Woo TG, Jeon WY, Park HH, Lee MH, Bae TS, et al. Surface characteristics of titanium anodized in the four different types of electrolyte. *Electrochim Acta* 2007;53:863–70.
- [28] Cigada A, Cabrini M, Pedferri P. Increasing of the corrosion resistance of the Ti6Al4V alloy by high thickness anodic oxidation. *J Mater Sci Mater Med* 1992;3:408–12.
- [29] Hanawa T, Ota M. Calcium phosphate naturally formed on titanium in electrolyte solution. *Biomaterials* 1991;12:767–74.
- [30] Yan WQ, Nakamura T, Kobayashi M, Kim HM, Miyaji F, Kokubo T. Bonding of chemically treated titanium implants to bone. *J Biomed Mater Res* 1997;37:267–75.
- [31] Yang B, Uchida M, Kim HM, Zhang X, Kokubo T. Preparation of bioactive titanium metal via anodic oxidation treatment. *Biomaterials* 2004;25:1003–10.
- [32] Ishizawa H, Ogino M. Characterization of thin hydroxyapatite layers formed on anodic titanium oxide films containing Ca and P by hydrothermal treatment. *J Biomed Mater Res* 1995;29:1071–9.
- [33] Kim HM. Ceramic bioactivity and related biomimetic strategy. *Curr Opin Solid State Mater Sci* 2003;7:289–99.
- [34] Kim HM, Himeno T, Kawashita M, Kokubo T, Nakamura T. The mechanism of biomineralization of bone-like apatite on synthetic hydroxyapatite: an in vitro assessment. *J R Soc Interface* 2004;1:17–22.
- [35] Juhasz JA, Best SM, Auffret AD, Bonfield W. Biological control of apatite growth in simulated body fluid and human blood serum. *J Mater Sci Mater Med* 2008;19:1823–9.
- [36] Das K, Bose S, Bandyopadhyay A. Surface modifications and cell-materials interactions with anodized Ti. *Acta Biomater* 2007;3:573–85.
- [37] Ponsonnet L, Reybier K, Jaffrezic N, Comte V, Lagneau C, Lissac M, et al. Relationship between surface properties (roughness, wettability) of titanium and titanium alloys and cell behaviour. *Mater Sci Eng C* 2003;23:551–60.
- [38] Kasemo B, Gold J. Implant surfaces and interface processes. *Adv Dent Res* 1999;13:8–20.